AWARD NUMBER: W81XWH-15-1-0728

TITLE: MYC RNAi-PT Combination Nanotherapy for Metastatic Prostate Cancer Treatment

PRINCIPAL INVESTIGATOR: Omid C. Farokhzad

CONTRACTING ORGANIZATION: Brigham and Women's Hospital
Boston, MA 02115

REPORT DATE: October 2017

TYPE OF REPORT: Annual

PREPARED FOR: U.S. Army Medical Research and Materiel Command
Fort Detrick, Maryland 21702-5012

REPORT DOCUMENTATION PAGE

Form Approved
OMB No. 0704-0188

1. REPORT DATE	2. REPORT TYPE	3. DATES COVERED
October 2017	Annual	30 Sep 2016 - 29 Sep 2017

4. TITLE AND SUBTITLE
MYC RNAi-Pt Combination Nanotherapy for Metastatic Prostate Cancer Treatment

5a. CONTRACT NUMBER

5b. GRANT NUMBER
W81XWH-15-1-0728

5c. PROGRAM ELEMENT NUMBER

6. AUTHOR(S)
Omid Farokhzad (initiating PI), Angelo De Marzo (partnering PI), Charles Bieberich (partnering PI), Srinivasan Yegnasubramanian (co-I), Jinjun Shi (co-I)

E-Mail: ofarokhzad@bwh.harvard.edu

5d. PROJECT NUMBER

5e. TASK NUMBER

5f. WORK UNIT NUMBER

7. PERFORMING ORGANIZATION NAME(S) AND ADDRESS(ES)

Brigham and Women's Hospital, Boston, MA 02115

University of Maryland, Baltimore County, Baltimore, MD 21250

The Johns Hopkins University School of Medicine, Baltimore, MD 21205

8. PERFORMING ORGANIZATION REPORT NUMBER

9. SPONSORING / MONITORING AGENCY NAME(S) AND ADDRESS(ES)

U.S. Army Medical Research and Materiel Command
Fort Detrick, Maryland 21702-5012

10. SPONSOR/MONITOR'S ACRONYM(S)

11. SPONSOR/MONITOR'S REPORT NUMBER(S)

12. DISTRIBUTION / AVAILABILITY STATEMENT

Approved for Public Release; Distribution Unlimited

13. SUPPLEMENTARY NOTES

14. ABSTRACT
The main objective of this project is to develop an innovative nanotherapy modality by combining platinum (Pt) chemotherapy and MYC-targeting RNA interference (RNAi) for more effective treatment of metastatic prostate cancer (PCa). In Year 2 of this project, we have made substantial accomplishments for the proposed tasks. We systematically evaluated the *in vivo* behaviors (*e.g.*, PK and BioD) of the NP platform (PDSA8-2 NPs) optimized in Year 1 of this project. The optimal NPs showed long blood circulation, and can efficiently deliver siRNA to PCa tumor tissues to inhibit MYC expression. We showed that the NP-mediated MYC silencing could significantly inhibit tumor growth in PCa xenograft model. We also successfully established Pt-resistant PCa cells and investigated the *in vitro* toxicity of the NPs loaded with MYC siRNA and cisplatin prodrug (synthesized in Year 1 of this project) against the Pt-resistant PCa cells. In parallel, we further characterized the phenotypic characteristics of the cell lines derived from sites of metastasis of MYC-driven transgenic BMPC tumors (established in Year 1 of this project), and employed the new cell line to evaluate the *in vitro* and *in vivo* MYC silencing by the optimal NPs. We demonstrated that the NP-mediated MYC silencing can significantly inhibit the proliferation of BMPC cells. We also did RNAseq to assess whether the MYC signature is being modulated in the BMPC mice and cell lines. Below are the accomplishments for each subtask.

15. SUBJECT TERMS
Nanotechnology, nanoparticle, siRNA delivery, platinum, MYC, prostate cancer, drug resistance, mouse model, pathology, genomics

16. SECURITY CLASSIFICATION OF:			17. LIMITATION OF ABSTRACT	18. NUMBER OF PAGES	19a. NAME OF RESPONSIBLE PERSON
a. REPORT	b. ABSTRACT	c. THIS PAGE			USAMRMC
Unclassified	Unclassified	Unclassified	Unclassified	26	19b. TELEPHONE NUMBER *(include area code)*

Table of Contents

Page

1. INTRODUCTION

The main objective of this project is to develop an innovative nanotherapy modality by combining platinum (Pt) chemotherapy and MYC-targeting RNA interference (RNAi) for more effective treatment of metastatic prostate cancer (PCa). Two specific aims are proposed in this study, including (i) development and optimization of MYC siRNA-Pt nanoparticles (NPs), and (2) determination of the efficacy of select NPs in the $B13^{MYC/Cre}|Pten^{fl/fl}$ engineered PCa mouse model. This project is directed by an interdisciplinary team in the PCa research field, including Initiating PI Dr. Omid Farokhzad from Brigham and Women's Hospital (BWH)/Harvard Medical School (HMS), Partnering PIs Dr. Charles Bieberich from the University of Maryland Baltimore County (UMBC) and Dr. Angelo De Marzo from the John Hopkins University (JHU), and two co-investigators (Dr. Srinivasan Yegnasubramanian from JHU and Dr. Jinjun Shi from BWH/HMS).

2. KEYWORDS

Nanotechnology, lipid, polymer, hybrid nanoparticle, siRNA delivery, platinum, MYC, prostate cancer, drug resistance, mouse model, pathology, genomics

3. ACCOMPLISHMENTS

- **What were the major goals of the project?**

The project has two specific aims. The major tasks and subtasks in the SOW are shown below.

Specific Aim 1: Development and optimization of MYC siRNA-Pt NPs
Major Task 1. Rational design and creation of siRNA-Pt NPs: (i) NP optimization for effective gene silencing; (ii) Synthesis of cisplatin prodrugs; and (iii) siRNA-Pt NP development
Major Task 2. In vitro evaluation and mechanism studies: (i) Cellular cytotoxicity of MYC siRNA-Pt NPs; and (ii) Mechanism study of the MYC role in Pt resistance
Major Task 3. In vivo test and optimization: (i) In vivo studies of select hybrid NPs; and (ii) In vivo evaluation of siRNA-Pt NPs

Specific Aim 2: Determination of the efficacy of select RNAi-Pt NPs in the $B13^{MYC/Cre}|Pten^{fl/fl}$ engineered PCa mouse model
Major Task 4. Evaluation of MYC silencing in the genetically engineered mouse model: (i) NP BioD and MYC silencing; and (ii) Assessment of a MYC gene expression signature to track pharmacodynamic response of MYC siRNA-Pt NP therapy
Major Task 5. Investigation of tumor development/progression to metastasis and side effects after NP administration: (i) Effect of MYC siRNA-Pt NPs on PCa progression to metastasis; (ii) Effect of siRNA-Pt NPs on survival in $B13^{MYC/Cre}|Pten^{fl/fl}$ males with late stage disease; and (iii) Side effects of the combination nanotherapy

- **What was accomplished under these goals?**

In Year 2 of this project (9/2016 - 9/2017), we have made substantial accomplishments for the proposed tasks. We systematically evaluated the in vivo behaviors (*e.g.*, PK and BioD) of the optimal NP platform (PDSA8-2 NPs) which was developed in Year 1 of this project. The optimal NPs showed long blood circulation, and can efficiently deliver siRNA to PCa tumor tissues to inhibit MYC expression. We showed that the NP-mediated MYC silencing can significantly inhibit tumor growth in PCa xenograft model. We also successfully established Pt-resistant PCa cells and investigated the in vitro toxicity of the NPs loaded with MYC siRNA and cisplatin prodrug (synthesized in Year 1 of this project) against the Pt-resistant PCa cells. In parallel, we further characterized the phenotypic characteristics of the cell lines derived from sites of metastasis of MYC-driven transgenic BMPC tumors (established in Year 1 of this project), and employed the new cell line to evaluate the in vitro and in vivo MYC silencing by the optimal NPs. We demonstrated efficient MYC silencing both in vitro and in vivo, and this NP-mediated MYC silencing can significantly inhibit the proliferation of the BMPC cells. We also did RNAseq to assess whether the MYC signature is being modulated in the BMPC mice and cell lines. Below are the accomplishments for each subtask.

Major Task 1. Rational design and creation of siRNA-Pt NPs
(i) NP optimization for effective gene silencing (Farokhzad and Shi, BWH)
We have completed this subtask in Year 1 of this project (9/2015 - 9/2016). We have designed and prepared a library of redox-responsive poly(disulfide amide) (PDSA)-based NPs. We have also extensively studied the effects of formulation parameters and lipid-PEGs on NP behaviors

in vitro and in vivo. By adjusting the polymer structure and NP formulation, we have finally obtained the optimal NP platform which is made with PDSA8-2 polymer (Figure 1a and 1b).

(ii) Synthesis of cisplatin prodrugs (Farokhzad and Shi, BWH)

In Year 1 of this project (9/2015-9/2016), we have designed and synthesized a series of cisplatin prodrugs and employed NMR to demonstrate the successful synthesis.

(iii) siRNA-Pt NP development (Farokhzad and Shi, BWH)

We have finished this subtask in Year 1 of this project. We chose PDSA8-2 NPs to encapsulate the cisplatin prodrugs and examined the encapsulation efficiency (EE%) and loading level (LL%). Because the prodrug with sebacic tails (named as Pt-8C, Figure 1c) shows highest EE% (~85.6%) and LL% (~9.4%), we used the PDSA8-2 NPs to co-encapsulate MYC siRNA and Pt-8C for the following tasks.

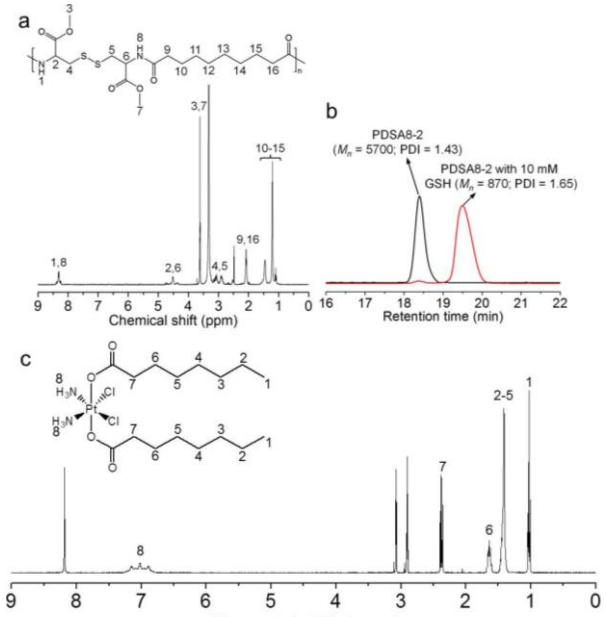

Figure 1. (a) Molecular structure and ^{1}HNMR spectrum of the PDSA8-2 polymer. (b) GPC profile of PDSA8-2 polymer before and after incubation with 10 mM GSH. (c) Molecular structure and ^{1}HNMR spectrum of cisplatin prodrug Pt-8C.

Major Task 2. In vitro evaluation and mechanism studies

(i) Cellular cytotoxicity of MYC siRNA-Pt NPs (Farokhzad and Shi, BWH)

In Year 1 of this project (9/2015-9/2016), we demonstrated that the PDSA8-2 NPs can efficiently deliver MYC siRNA to PCa cell line (PC3 cells) and silence MYC expression (Figure 2a and 2b). In Year 2, we have used these NPs to encapsulate Pt-8C and then studied the cytotoxicity of Pt-8C loaded PDSA8-2 NPs against PC3 cells. Figure 2c shows the viability of PC3 cells incubated with the drug loaded NPs for 24 h. The half maximal inhibitory concentration (IC50) of free cisplatin is around 3.9 mg/L while that of Pt-8C loaded NPs showed an IC50 of ~9.2 mg/L. Based on the results of MYC silencing and cytotoxicity assay, we then examined the influence of MYC siRNA and Pt-8C co-loaded NPs (named as MYC-Pt NPs) on the proliferation of PC3 cells (Figure 2d). The MYC-Pt NPs can significantly inhibit the cell proliferation and there is less than 2-fold increase in the number of the cells

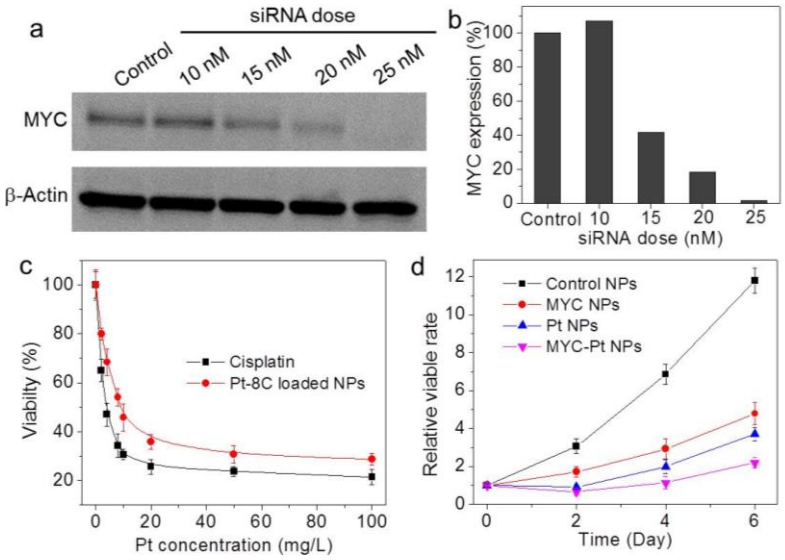

Figure 2. (a, b) Western blot analysis of MYC expression in PC3 cells treated with MYC siRNA loaded PDSA8-2 NPs. (c) Cytotoxicity of cisplatin and Pt-8C loaded PDSA8-2 NPs against PC3 cells; (d) Proliferation profile of PC3 cells treated with MYC siRNA loaded (MYC NPs), Pt-8C loaded (Pt NPs), and MYC siRNA and Pt-8C co-loaded (MYC-Pt NPs) PDSA8-2 NPs. siRNA concentration is 20 nM; Pt concentration is 4.2 mg/mL; Luciferase siRNA loaded NPs are used as control.

treated with 20 nM MYC siRNA and 4.2 mg/L Pt. In comparison, there is around 4-5-fold increase in the number of the cells treated with the NPs only loading MYC siRNA (20 nM) or Pt (4.2 mg/L). Currently, we are optimizing the MYC-Pt NPs and testing the influence of different doses of cisplatin prodrugs and MYC siRNA on the inhibition of the PC3 cell growth.

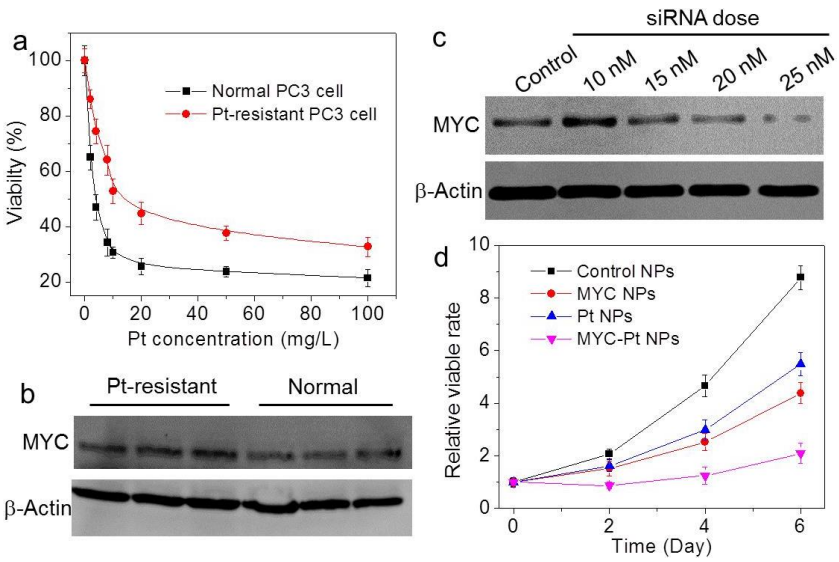

Figure 3. (a) Cytotoxicity of cisplatin against naive and Pt-resistant PC3 cells. (b) Western blot analysis of MYC expression in the normal and Pt-resistant PC3 cells. (c) Western blot analysis of MYC expression in the Pt-resistant PC3 cells treated with the MYC-Pt NPs. (d) Proliferation profile of the Pt-resistant PC3 cells treated with the MYC-Pt NPs and the NPs only loading MYC siRNA (MYC NPs) or Pt-8C (Pt NPs). siRNA concentration is 20 nM; Pt concentration is 4.2 mg/mL; Luciferase siRNA loaded NPs are used as control.

(ii) Mechanism study of the MYC role in Pt resistance (Farokhzad and Shi, BWH; De Marzo, JHU)

In this subtask, we first established Pt-resistant PC3 cells and then investigated whether the MYC silencing can re-sensitize Pt-resistant PC3 cells to the treatment with cisplatin. To establish the Pt-resistant cells, PC3 cells were incubated in the culture medium containing cisplatin. According to the cytotoxicity of cisplatin shown in Figure 2c, the initial cisplatin concentration was set as 0.39 mg/L (1/10 of the IC50 of cisplatin against PC3 cells) and the drug-resistant cells were successfully established via gradually increasing the cisplatin concentration in the culture medium. Figure 3a shows the cytotoxicity of cisplatin against normal and Pt-resistant PC3 cells. The IC50 of cisplatin against Pt-resistant cells is around 14.1 mg/L, which is around 4-fold higher than that of cisplatin ag ainst the normal PC3 cells (~3.9 mg/L). Moreover, compared to the parental cells, Pt-resistant cells show higher MYC expression (Figure 3b). We next investigated whether the MYC silencing can re-sensitize the cells to the treatment with cisplatin. Figure 3c shows the MYC expression in the Pt-resistant cells treated with the MYC-Pt NPs. These co-delivery NPs can efficiently knock down MYC expression in the Pt-resistant cells. With this MYC silencing, the Pt-resistant cells became sensitive to cisplatin and there is only around 2-fold increase in the number of the cells treated with the MYC-Pt NPs (Figure 3d). In comparison, there is more than 4-fold or 5-fold increase in the number of the cells treated with the NPs only loading MYC siRNA (20 nM) or Pt (4.2 mg/L), respectively. We are now optimizing the MYC-Pt NPs by testing different doses of cisplatin prodrugs and MYC siRNA in cytotoxicity studies with Pt-resistant PC3 cells. Simultaneously, the Pt-resistant cells will be given to Drs. De Marzo and Yegnasubramanian at JHU for RNAseq analysis.

Major Task 3. In vivo test and optimization

(i) In vivo studies of select hybrid NPs (Farokhzad and Shi, BWH; De Marzo, JHU)

In this subtask, we first assessed the pharmacokinetics (PK) of the siRNA loaded PDSA8-2 NPs. PK was examined by intravenous injection of DY677-siRNA loaded NPs to normal Balb/c mice (1 nmol siRNA dose per mouse, n = 3). Figure 4a shows that the naked siRNA is rapidly cleared

from the blood and its blood half-life ($t_{1/2}$) is less than 10 min. In contrast, due to the protection of PEG outer layer, the siRNA loaded NPs show long blood circulation with a $t_{1/2}$ of ~4.92 h. We next examined the biodistribution (BioD) of the siRNA loaded NPs. The BioD was evaluated by intravenously injecting DY677-siRNA loaded NPs into athymic nude mice bearing PC3 xenograft tumors. Figure 4b shows the fluorescent image of the mice at 24 h post injection, showing a much higher tumor accumulation of the siRNA NPs than naked siRNA (Figure 4b and 4c). We further harvested the tumors and major organs at 24 h post injection (Figure 4d and 4e) and the quantification of BioD is shown in Figure 4f. The siRNA loaded NPs show about 6-fold higher accumulation in tumors than naked siRNA.

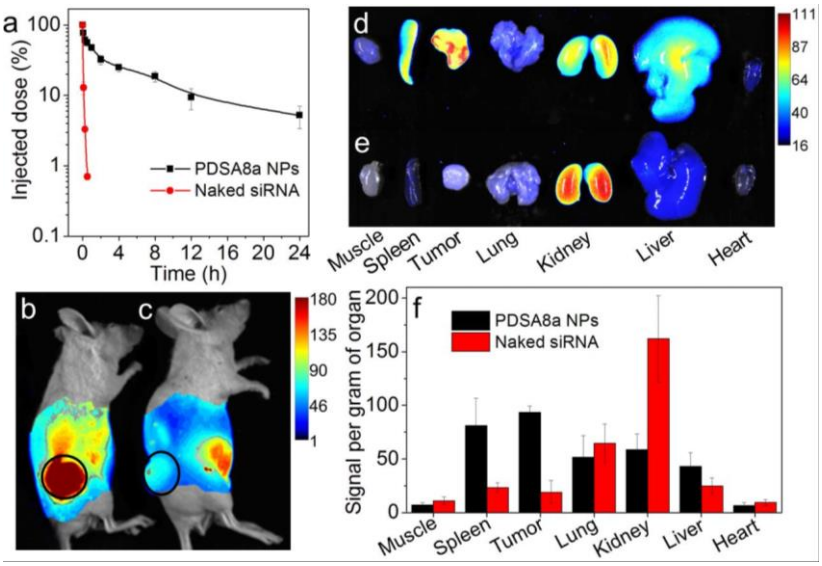

Figure 4. (a) PK of naked siRNA and siRNA loaded NPs. (b, c) Overlaid fluorescent image of the PC3 xenograft tumor-bearing nude mice at 24 h post injection of siRNA loaded NPs (b) and naked siRNA (c). Tumors are indicated by ellipses. (d, e) Overlaid fluorescent image of the tumors and main organs of the PC3 xenograft tumor-bearing nude mice sacrificed at 24 h post injection of the siRNA loaded NPs (d) and naked siRNA (e). (f) Biodistribution of the NPs quantified from (d, e).

With these promising in vitro and PK/BioD results described above, we further evaluated whether the siRNA loaded PDSA8-2 NPs can silence MYC expression in vivo. To this end, the siRNA loaded NPs were intravenously injected into the PC3 xenograft tumor-bearing athymic nude mice (1 nmol siRNA dose per mouse, n = 3) for three consecutive days. Figures 5a and 5b show that the administration of the MYC siRNA loaded NPs lead to ~55% knockdown in MYC protein expression compared to the control NPs. Immunohistochemical (IHC) analysis (Figure 5c) also demonstrated decreased MYC expression in the tumor tissue of the mice treated with the MYC siRNA loaded NPs.

We also evaluated the potential in vivo side effects of the PDSA8-2 NPs. The NPs loaded with MYC siRNA were intravenously injected to normal Balb/c mice (1 nmol siRNA dose per mouse, n = 3). Blood serum analysis shows that TNF-α, IFN-γ, IL-6, and IL-12 levels were in the normal range at 24 h post injection of the MYC siRNA loaded NPs (Figure 6). After three daily injections, no

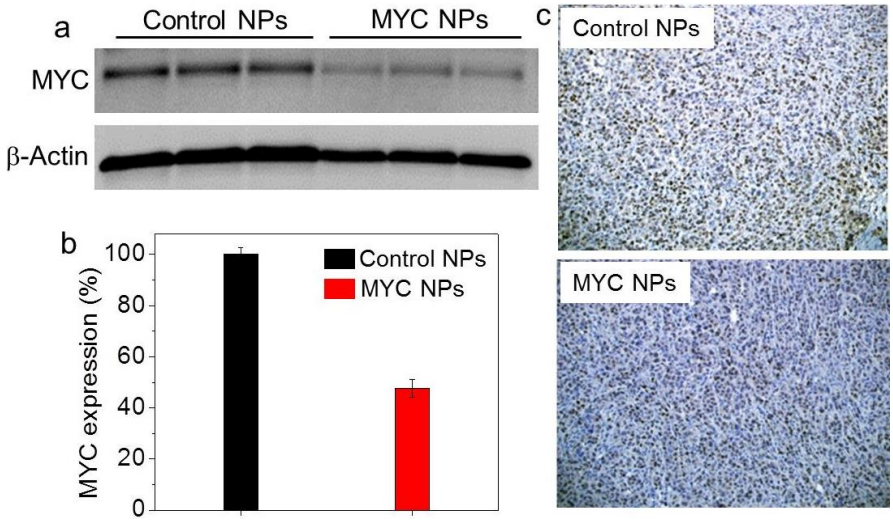

Figure 5. Western blot (a, b) and IHC (c) analysis of MYC expression in the PC3 xenograft tumor tissue after systemic treatment by control NPs and MYC siRNA loaded NPs. Luciferase siRNA loaded NPs are used as control.

noticeable histological changes were noticed in the tissues from heart, liver, spleen, lung or kidney (Figure 7). These results indicate the good biocompatibility of the PDSA8-2 NP platform used in this project.

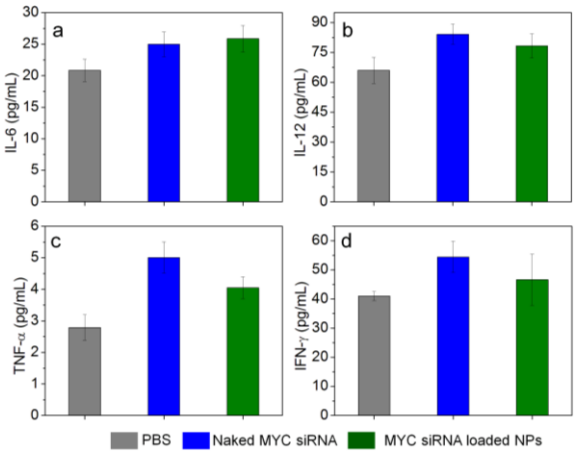

Figure 6. Serum levels of IL-6 (a), IL-12 (b), TNF-α (c), and IFN-γ (d) at 24 h post injection of PBS, naked MYC siRNA, and MYC siRNA loaded NPs.

(ii) In vivo evaluation of siRNA-Pt NPs
(Farokhzad and Shi, BWH; De Marzo, JHU)

We next evaluated whether the NP-mediated MYC silencing has an anticancer effect. The MYC siRNA loaded NPs were intravenously injected into the PC3 xenograft tumor-bearing mice once every two days at a 1 nmol siRNA dose per mouse (n = 5). Figure 8 shows that the NP-mediated MYC silencing has an impressive anticancer effect. After 5 intravenous injections of the siRNA loaded NPs into PC3 xenograft tumor-bearing mice, the tumor growth rate is efficiently inhibited. A 3.5-fold increase in tumor size (from ~70 to 278 mm^3) was observed at day 22 in mice treated with the MYC siRNA loaded NPs. In contrast, there is around 8-fold increase in the tumor size of the mice treated with PBS, naked MYC siRNA, or control NPs.

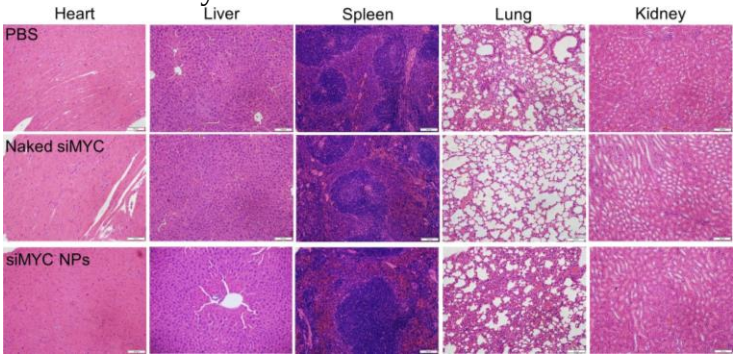

Figure 7. Histological sections of the major organs of mice intravenously injected with PBS, naked MYC siRNA, and MYC siRNA loaded NPs. Hematoxylin-eosin; magnification 100 ×.

Currently, we are planning the in vivo anticancer effect of the MYC-Pt NPs using naïve and Pt-resistant PC3 xenograft tumor models.

Major Task 4. Evaluation of MYC silencing in the genetically engineered mouse model:

(i) NP BioD and MYC silencing
(Bieberich, UMBC; De Marzo; and Yegnasubramanian JHU; Farokhzad and Shi, BWH)

Further characterization of BMPC1 and BMPC2 cell lines derived from sites of metastasis of MYC-driven BMPC tumors:

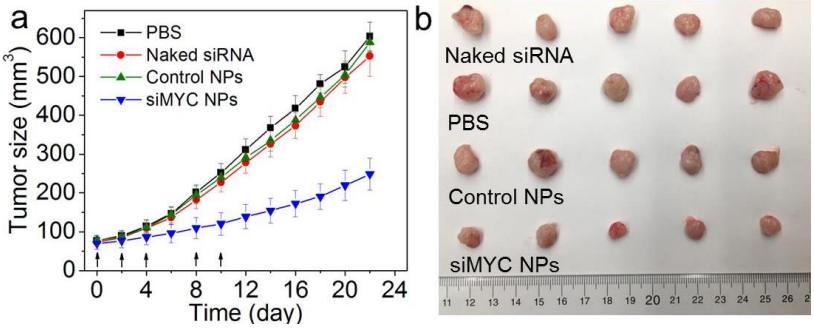

Figure 8. (a) Tumor growth of the PC3 xenograft tumor-bearing nude mice (n = 5) after IV treatment by PBS, naked MYC siRNA, control NPs, and MYC siRNA loaded NPs. The IV injections are indicated by the arrows. (b) Photograph of the harvested PC3 xenograft tumors after 22 day evaluation of the mice in (a). Luciferase siRNA loaded NPs are used as control.

We have further characterized the phenotypic characteristics of these cells in which each cell line was initially examined using immunohistochemistry (IHC) and RNA in situ hybridization (RNAish) on cells that were fixed in formalin and embedded into paraffin blocks (formalin fixed and paraffin embedded or FFPE), as well as by RNAseq. **Figure 9** shows that MYC protein by IHC was detected at high levels whereas Pten was absent in both cell lines, consistent with the

trigenic model. To confirm prostatic origin, we examined the expression of Nkx3.1, Hoxb13, and AR. Both BMPC1 and BPMC2 had detectable levels of Nkx3.1 mRNA and protein as well as Hoxb13 mRNA. AR protein was detected at low levels in both the cytoplasm and nucleus of BMPC1 cells. Strong nuclear staining and localization of AR was not observed in the BMPC1 cell line under normal tissue culture conditions. BMPC2 cells did not have detectable levels of AR protein by IHC. AR mRNA was readily detected in BMPC1 cells and was essentially undetectable in BMPC2 cells. Epithelial markers (i.e. keratin 18 and Foxa1) were positive across BMPC1 and BMPC2 and Foxa2, a determinant of neuroendocrine prostate cancer, was not detected (not shown). Also absent was the basal cell marker, P63 (not shown). A standard Giemsa stained karyotype for BMPC1 and BMPC2 was performed (**Figure 9c**). BMPC1 is a male murine cell line with a modal number of chromosomes ranging from 72-80. In addition to numerical aberrations, small fragments and chromosome associations were observed. Deletion of chromosome 20 and an internal duplication of chromosome 1 were shared across both cell lines. BMPC2 is also a male murine cell line with a modal range of chromosomes from 52 to 102. BMPC2 demonstrated a higher tendency for chromosome associations and fusions between centromeres, telomeres, and other chromosomes.

A.

	BMPC1	BMPC2
Protein		
AR	+ weak, cytoplasmic	-
NKX3.1	+	+
c-MYC	++	++
Pten	-	-
Ker 18	+	+
Ker 5	-	-
Foxa1	+	+
Foxa2	-	-
P63	-	-
mRNA		
AR	++	-
NKX3.1	+	+
c-MYC	++	++
Hoxb13	+	+
TERC	+	++
45S	++	++

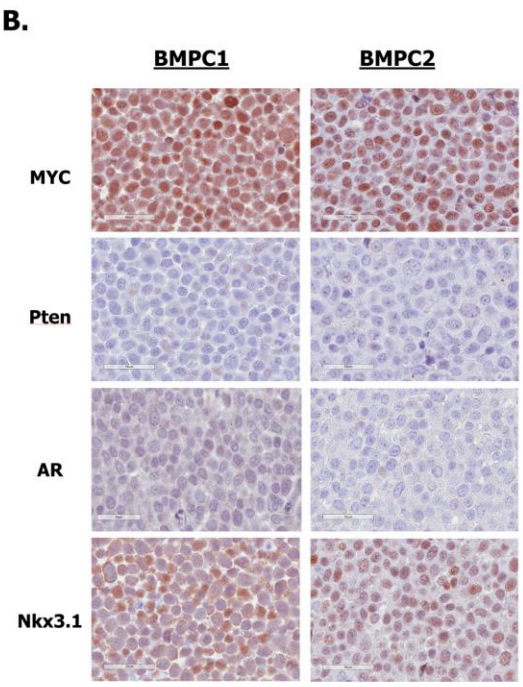

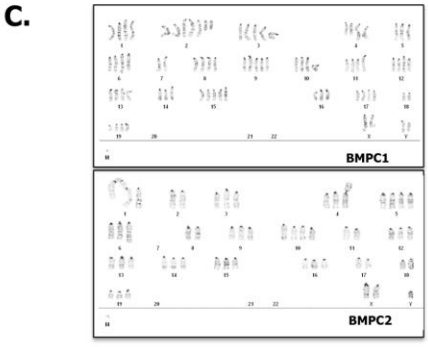

Figure 9. Molecular and Genetic Characterization of Murine Cell Lines, BMPC1 and BMPC2. A. Summary of IHC and RNAish staining results delineating tissue of origin and cell subtype. (- = negative, + = low, ++ = high). B. IHC staining of key proteins involved in prostate carcinogenesis and disease progression. ker 5 = keratin 5; ker 18 is keratin 18. C. Standard karyotype of BMPC1 (top) and BMPC2 (bottom).

Since BMPC1 cells expressed AR mRNA yet very little AR protein, which was not concentrated within nuclei, we hypothesized that AR protein in BMPC1 cells may be unstable and rapidly degraded in the absence of ligand. In an effort to stabilize AR protein and induce nuclear translocation, we treated BMPC1 cells with increasing doses of the synthetic androgen,

R1881, following serum starvation. By western blot, AR protein was detectable in the BMPC1

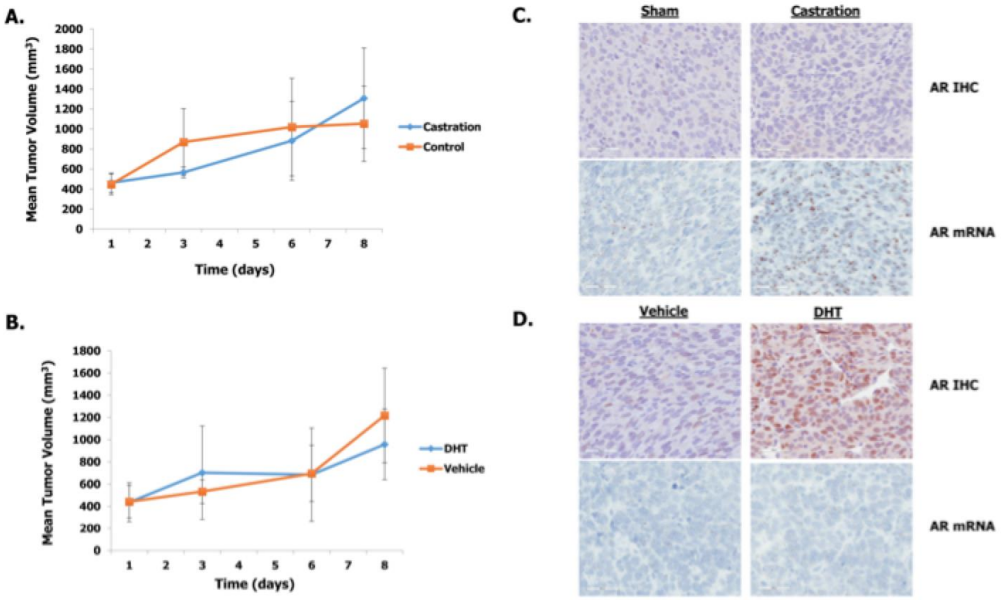

Figure 10. In Vivo Effect of Castration and DHT Supplementation on BMPC1 Allograft Growth and AR Expression in Nude Mice. Nude mice were inoculated with BMPC1 and grown to 500cc3. A. Mice underwent sham castration or castration and tumor volume was measured daily until euthanasia. No effect of castration was observed (P >0.05 across all time points). B. Empty or DHT-containing silastic tubing was placed subcutaneously in BMPC1 bearing nude mice. Tumor volume was measured daily until euthanasia. DHT did not increase allograft growth (P>0.05 across all time points). C. AR mRNA levels increased following castration. No change in AR protein was observed. D. AR protein levels were increased in the presence of DHT and localized to the nucleus. No change in AR mRNA was detected.

cell line following exposure to androgen (Not shown). Using IHC on FFPE cell pellets, we confirmed an R1881-induced increase in AR protein in BMPC1 cells and observed nuclear translocation of the receptor (Not shown). We next performed in vivo studies assessing the androgen responsiveness of the BMPC1 cell line in allografts in immunocompromised mice, given the in vitro increase of AR protein levels in the presence of R1881. BMPC1 allografts were allowed to grow in nude mice to a tumor volume of 500 mm3 before beginning treatment. Initially, we evaluated BMPC1 allograft growth following castration. To control for an effect of systemic inflammation and iatrogenic stress, control animals underwent a sham castration. No significant effect on BMPC1 allograft growth was observed following castration (n=5) over an 8 day time course compared to the sham control (n=3) (**Figure 10**). Since AR protein was stabilized in the presence of the AR agonist in our in vitro studies, we measured BMPC1 allograft growth after the addition of DHT. Silastic tubing containing DHT (n=5) or blank tubing (n=5) was placed subcutaneously in the tumor-bearing mice on Day 0. No significant difference in BMPC1 allograft volume was observed between either group, similar to the results of the castration experiment (**Figure 10b**). At necropsy, BMPC1 allografts from the DHT and castration experiments were formalin-fixed and paraffin embedded for further study of AR expression. Following castration, AR mRNA levels in the allografts increased relative to both control (no surgery) and sham specimens (**Figure 10c**). IHC staining for AR protein remained virtually undetectable irrespective of castration status. Mice that harbored DHT-containing or blank silastic tubing (which were not castrated) had AR mRNA levels that did not change in the presence of DHT (**Figure 10d**). As in the cell lines treated with R1881 in vitro, AR protein was

readily detected in BMPC-1 allografts from DHT-treated mice and located in the nucleus. These characterizations will facilitate additional experiments to be carried out in year 3 using the BMPC1 allografts to detect effects on nanoparticle carried RNAi mediated MYC knockdown.

MYC knockdown in BMPC allograft tumors:

Prior to evaluating the MYC knockdown in BMPC allograft tumors, we first examined the NP-mediated MYC silencing in the BMPC1 cells. Figure 9 shows the MYC expression in the BMPC1 cells treated with the MYC siRNA loaded PDSA8-2 NPs. The siRNA loaded NPs can efficiently knock down MYC expression (Figure 11a). Particularly, there is extremely low MYC expression at 40 nM siRNA dose (Figure 11b). With this MYC silencing, the proliferation rate of the BMPC1 cells is significantly inhibited. Dose-dependent inhibition of cell growth was observed under 10, 20 and 40 nM treatment conditions over the six-day observation period. Impressively, there is nearly no increase in the number of the cells treated with the NPs at 40 nM siRNA dose (Figure 11c). In contrast, there is around 30-fold increase in the cell number treated with the control NPs.

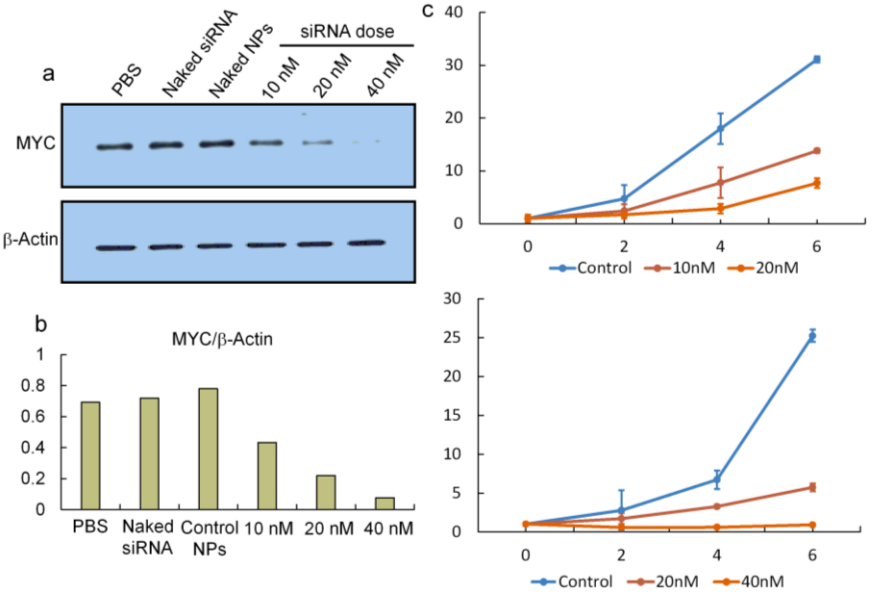

Figure 11. (a, b) Western blot analysis of MYC expression in BMPC1 cells treated with MYC siRNA loaded NPs. (c) Proliferation profile of BMPC1 cells treated with MYC siRNA loaded NP. Luciferase siRNA loaded NPs are used as control.

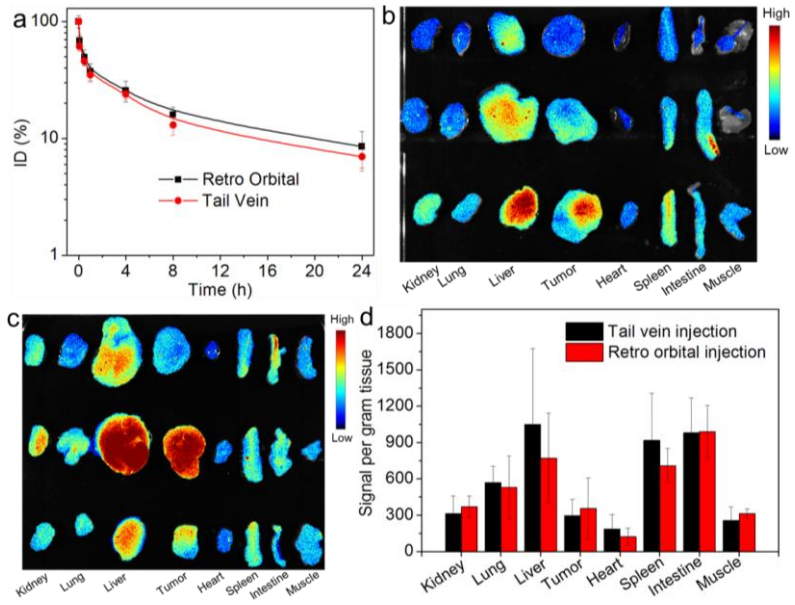

Figure 12. (a) PK of siRNA loaded NPs administrated via tail vein and retro-orbital injections. (b, c) Overlaid fluorescent image of the tumors and main organs of the BMPC allograft tumor-bearing nude mice sacrificed at 24 h post tail vein (b) or retro-orbital (c) injection of the siRNA loaded NPs. (d) Biodistribution of the NPs quantified from (b, c).

With the efficient in vitro MYC silencing in the BMPC1 cells, we next established BMPC allograft tumor-bearing mice model and evaluated the in vivo MYC silencing efficacy. To obtain the mice model, 1×10^6 BMPC1 cells were implanted into the flank of athymic nude mice. When BMPC1 tumors reached ~100 mm^3, MYC siRNA loaded NPs were administrated via retro-orbital injection at 24 h intervals for three consecutive days. On day four, the mice were euthanized and tumors were resected. Where feasible, the tumors were divided in half for

western blot and histological quantification of MYC accumulation. Noting that, because we administrated the NPs via tail vein injection in Major Task 3, we investigated the PK and BioD of the siRNA loaded NPs which were administrated via tail vein and retro-orbital injections. The data in Figure 12 demonstrate that there is no significant difference in the PK and BioD of the NPs administrated via tail vein or retro-orbital injection.

Two additional experiments beyond what was presented in year 1 progress report were carried out in year two and both show efficacy in knocking down MYC protein in vivo. In the

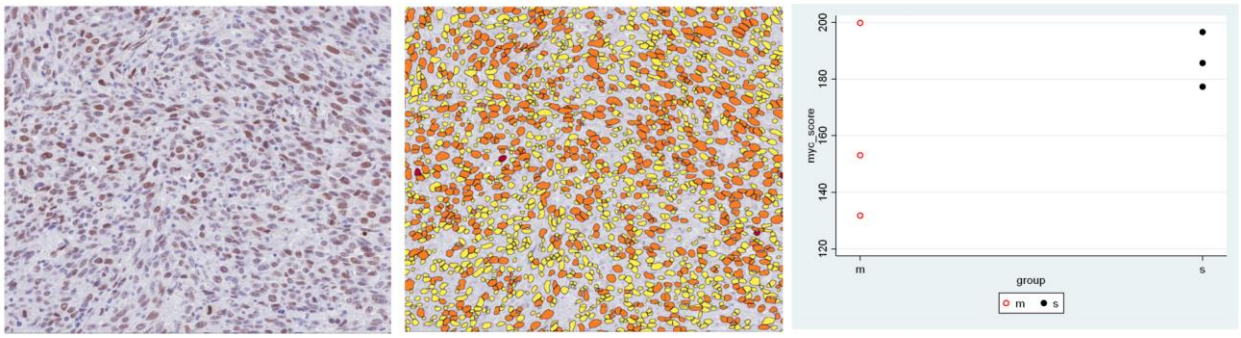

Figure 13. Aperio computerized image analysis results from same experiment show in in Figure 1. Left most panel show example of MYC staining and middle shows Aperio identification of nuclei stained at 3 different intensities. The intensities were used to generate an "H-score", which is graphed on the right most pane. M = MYC targeted and s = control targeted particles.

first experiment, 1×10^6 cells in DMEM were injected subcutaneously into the flank of athymic nude mice (N=6). When BMPC1 tumors reached ~100 mm^3, 200 µl MYC-RNAi NPs (5 uM) was delivered via the tail vein at 48-hour intervals over 10 days. On day 11 (24 hours after the fifth injection), the mice were euthanized and tumors were resected. The tumors were divided

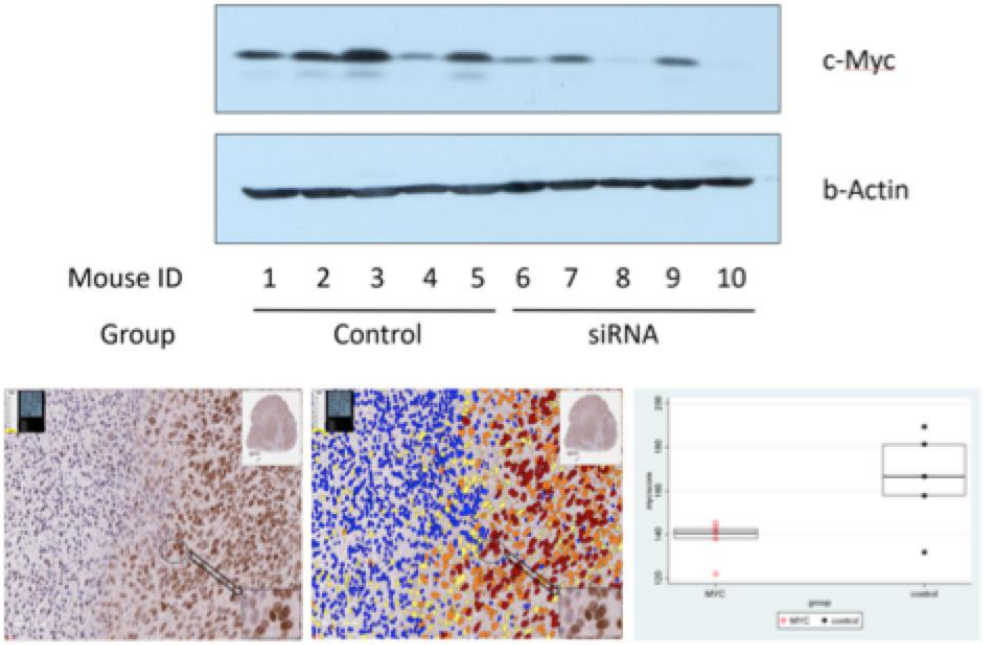

Figure 14. Western blot (top panels) and Aperio computerized image analysis (bottom panels) results from experiment 2. Control in western blot is the non-targeted siRNA nano particle treated group and the siRNA is the MYC-targeted group. For the Aperio image analysis, in this experiment each cell in the tumor was assigned a value with either very low/zero intensity (blue cells) or 3 different positive staining intensifies (red are most intensely stained cells) used to generate an "H-score".

into parts for Western blot and histological quantification of MYC accumulation. MYC IHC was performed and whole slides were scanned and analyzed using Aperio software for computerized image analysis. Figure 13 shows an example of the MYC protein IHC staining and graphs of the image analysis derived score for the MYC staining, which shows apparent decreased staining in two of three mice analyzed in the MYC targeted group vs. the control group.

A second experiment was carried out with 10 mice as described for the first experiment described above, except that the mice received a total of seven NP injections over 14 days and were euthanized on day 15. The results are shown in Figure 14 show a clear decrease in MYC protein levels by Western blotting. When we examined the IHC based image analysis for the MYC protein score, the results were statistically significantly different for the MYC-targeted vs. control siRNA treated animals ($p = 0.036$, t-test). Currently, we are evaluating the influence of MYC silencing on the inhibition of the BMPC allograft tumor growth. In addition, we will also examine the effect of MYC-Pt NPs on the inhibition of the BMPC allograft tumor growth.

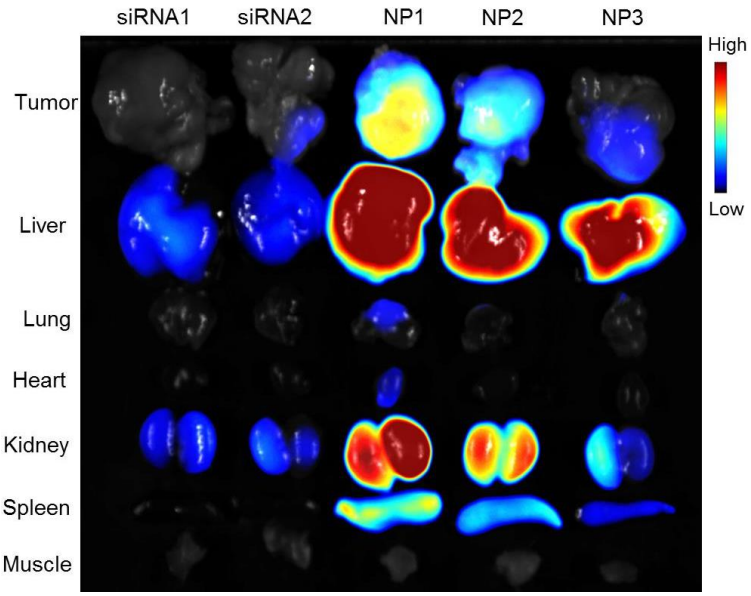

Figure 15. Overlaid fluorescent image of the tumors and main organs of the primary PCa tumor-bearing GEM mice sacrificed at 24 h post injection of the siRNA loaded NPs. The siRNA was labeled by fluorescent dye Cy7

To further test the NP accumulation in GEM model, we intravenously injected the siRNA (labeled by Cy7) loaded PDSA8-2 NPs to the GEM mice bearing primary tumors. Figure 15 shows the BioD of the siRNA loaded NPs after two consecutive injections. The siRNA loaded NPs show much higher accumulation in the primary tumor tissues than that of the naked siRNA. We are now repeating this experiment and evaluating the MYC silencing in the primary tumor tissues by injecting the MYC siRNA loaded PDSA8-2 NPs. In addition, we will also examine the effect of MYC-Pt NPs on the inhibition of the primary tumor growth.

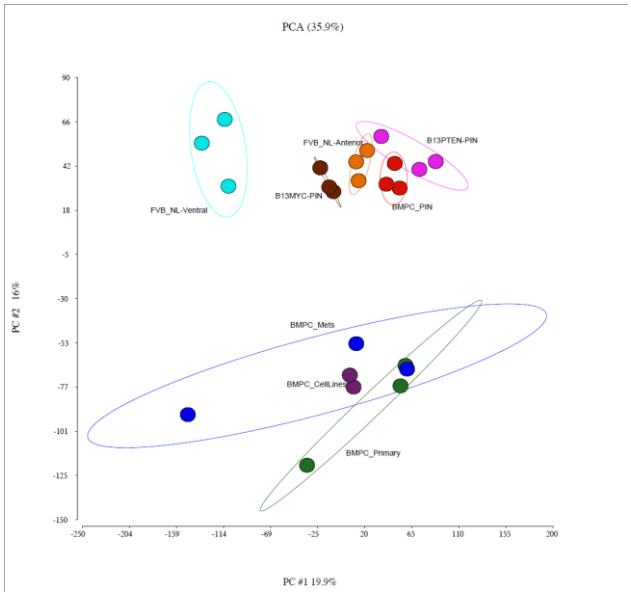

Figure 16. Principle Component's Analysis of the RNAseq Data from wild type (FBV) mice from the anterior and ventral lobes; PIN lesions from those driven by MYC alone (B13MYC-PIN), those driven by Pten loss alone (B13PTEN-PIN), those drive by combined Pten loss and MYC overexpression (BMPC_PIN), invasive BMPC primary tumors (BMPC_Primary) and metastatic lesions (BMPC_mets) from 3 mice each.

(ii) *MYC signature analysis in BMPC mice* (Yegnasubramanian and De Marzo, JHU; Bieberich, UMBC)

In order to assess whether our MYC signature is being modulated in the BMPC mice

and cell lines in our upcoming studies, we have further analyzed our RNAseq using 3 animals each for wildtype FVB ventral and anterior prostate lobes as well as *Hoxb13-MYC alone*, *Hoxb13-Cre|Pten*$^{Fl/Fl}$or BMPC = *Hoxb13-MYC|Hoxb13-Cre|Pten*$^{Fl/Fl}$, for a total of 21 samples across all stages of disease including normal, PIN, invasive primary adenocarcinoma and metastatic disease, as well as, in the two new BMPC metastatic cell lines. In order to determine how the MYC signature behaves in these different disease types we have performed additional bioinformatics analyses. Figure 16 shows a principle's component analysis (PCA) plot of the RNA-seq data. The results shows that the biological replicates of the non-malignant tissue are very consistent, while the primary and metastatic lesions have some biological variability.

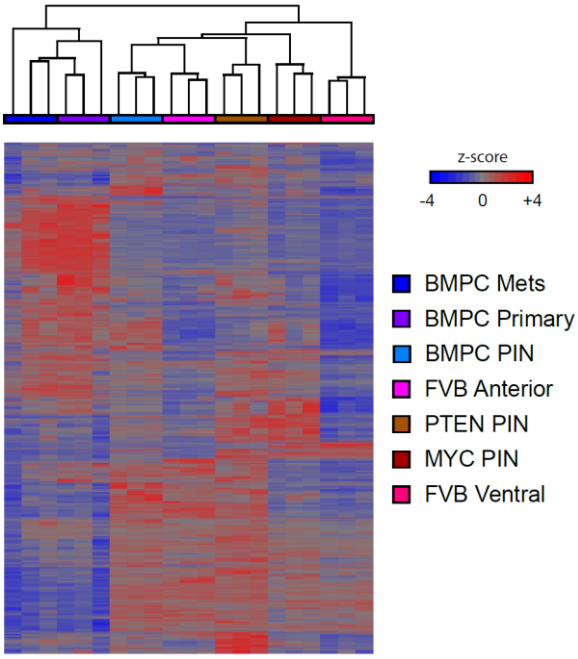

Figure 17. Heat Map from RNAseq data from same mouse groups as in Figure 13. Genes that were variably expressed across the groups using an ANOVA model, at a false discovery rate of 0.01, are plotted. Note large group of genes expressed in left most columns in red near the top that represent genes overexpressed in invasive adenocarcinomas and metastases, as compared to all other groups.

PC1 mainly discriminates differences in mouse lobes and PC2 appears to discriminate non-malignant from malignant including the two cell lines that we have produced from metastatic samples of different BMPC mice. Figure 17 shows a heatmap consisting of the genes that vary most across all of the RNAseq samples shown. These are gene level (not isoform level) values. The data shows a robust induction of a group of genes in the invasive lesions, as compared with the 3 different types of PIN lesions and the normal prostate lobes. In further work, we will identify the differentially expressed genes and pathways involved, and compare to our MYC signature, which will provide a basis for examining the effect of the nanoparticle treatments on the MYC signature by RNAseq, which we plan to do in year 3.

In anticipation of in vivo MYC siRNA-NP experiments in the BMPC GEM model in Year 3, we have been actively maintaining a breeding colony of BMPC mice throughout Years 1 & 2. In an effort to achieve maximal efficiency, we had adopted a breeding scheme that favored Hoxb13-MYC^{+}/Hoxb13-Cre^{+}/Pten$^{Fl/Fl}$ X MYC^{+}/Hoxb13-Cre^{+}/Pten$^{Fl/Fl}$ crosses. Careful monitoring of the prostate adenocarcinoma phenotype in BMPC males resulting from these crosses revealed a trend toward later emergence of disease. In addition, histopathological analyses revealed that ~20% of BMPC prostate tumors showed evidence of sarcomatoid features that were not observed in previous generations. To overcome this apparent phenotypic drift, we re-derived the BMPC model by breeding each of the parental Hoxb13 BAC transgenic strains (Hoxb13-Cre and Hoxb13-MYC) back to FVB/N (Jackson) for three generations, then

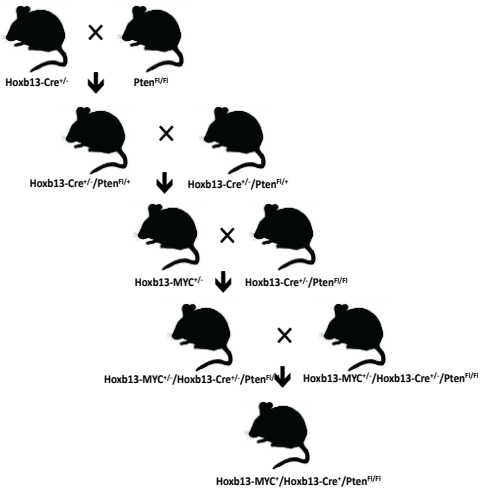

Figure 18. Standardized breeding scheme for production of BMPC males.

intercrossing with our Pten$^{FL/FL}$ strain. We then established a standardized breeding scheme (Figure 18) and generated a cohort of BMPC males.

To follow disease progression, we developed a prostate palpation protocol whereby each BMPC male is monitored weekly for emergence of disease. Using this protocol, the progression from normal to hyperplastic prostates can be readily be discerned as an increase in firmness of the gland. The next detectable stage is the emergence of BB-sized nodules, followed by a tumor of <0.5 g. As tumor progression ensues, tumor size can be reproducibly estimated in 0.5 g increments up to 5 g (max permitted under current approved IACUC protocol). Using this system, we monitored nine males generated under the standardized breeding scheme shown in Figure 19. The BMPC males generated under the standardized breeding scheme showed remarkably consistent disease progression. Histological analyses revealed that all nine animals had 100% adenocarcinoma with no evidence of sarcomatoid features.

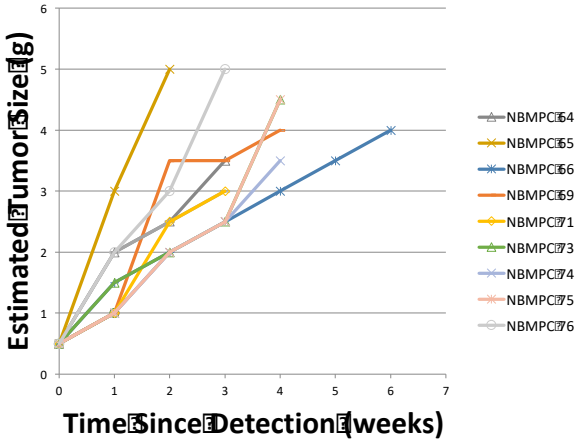

Figure 19. Disease progression in BMPC males monitored by palpation. Tumor size from 0.5 g until criteria for euthanasia were reached were plotted.

- **What opportunities for training and professional development has the project provided?**

While the Brigham and Women's Hospital (BWH) does not have an institutional policy requiring individual development plans for postdoctoral fellows and graduate students, the hospital is very committed to training its students and fellows to meet their research and career goals. The hospital supports a centralized career development office, *Office for Research Careers of BWH Brigham Research Institute*, which offers seminars ranging from career development to responsible conduct of research to how to secure NIH and other external funding. The office also addresses the specific needs of postdoctoral fellows and faculty investigators in the research community at BWH, and supports BWH researchers across the academic continuum, by providing resources to support career and professional development, by encouraging professional responsibility, enhancing the training experience and fostering effective mentoring. As a teaching affiliate of Harvard Medical School, BWH students and fellows have access to career development and support services offered by Harvard. Within my group, the postdoctoral fellows and students have routine meetings with me to discuss research project, skill and career development, and other needs they may have, and they present research work in the biweekly group meeting. The postdoctoral fellows and students are also encouraged and supported to attend local seminars, workshops, national conferences, and advanced education courses to present their research work, interact with colleagues, and enhance professional knowledge and skills, all of which will be helpful for their career development.

At Johns Hopkins there are a number of excellent opportunities for the professional development of our trainees related to this project. The pathology fellow is learning the histopathology of our prostate cancer mouse models and xenografts and also learning about IHC staining, in situ

hybridization, automated whole slides scanning and digital image analysis. Also, one of our oncology fellows has been central in developing and characterizing the BMPC cell lines in which he has been involved in cell culture, cell cloning and phenotyping. We meet weekly with the pathology and oncology fellows in which we discuss their research and they present results. Also, we hold weekly and biweekly lab meeting with other collaborating labs, including Drs. Yegnasubramanian's lab. In terms of bioinformatics opportunities, Dr. Yegnasubramanian is mentoring a number of trainees who are working on the RNAseq data analysis and gene signatures. All trainees also have access to a number of lectures on cancer including our Fall Course on Cancer Biology given in the oncology department that meets twice per week and covers major topics related to cancer biology and treatment. Dr. Bieberich holds weekly meetings with his participating students and they are afforded a number of excellent opportunities. Drs. Bieberich, De Marzo and Yegnasubramanian hold periodic meetings to discuss the project and fellows and students often take part in these discussions.

- **How were the results disseminated to communities of interest?**

Nothing to report.

- **What do you plan to do during the next reporting period to accomplish the goals?**

During the next reporting period, we will (i) further optimize the RNAi-Pt NPs by testing different doses of cisplatin prodrugs and MYC siRNA in cytotoxicity studies with Pt-naïve and Pt-resistant PCa cells; and (ii) evaluate the therapeutic efficacy of MYC-Pt NPs in PC3 cell line-based xenograft and BMPC allograft models.

At UMBC, we will receive MYC-Pt NPs from Dr. Farokhzad's laboratory and continue to perform the GEM model experiments with delivery of NPs for the studies outlined.

At JHU, we will continue to review all histopathology and perform immunohistochemistry and image analysis on the samples of NP treated animals performed in Dr. Bieberich's laboratory. With Dr. Yegnasubramanian's leadership we will be continue to derive the MYC signatures and apply them to RNA isolated from the NP treated animal tissues to develop a pharmacodynamics marker panel to complement MYC IHC staining and western blotting as a readout of whether the NPs have hit their target (e.g., MYC).

4. IMPACT

- **What was the impact on the development of the principal discipline(s) of the project?**

We have successfully designed and developed a new generation of lipid-polymer hybrid nanoparticles (NPs) with surface-tunable and redox-responsive properties. This unique NP platform is likely to make an impact on the field of RNA interference (RNAi), which holds significant potential for cancer therapy but requires effective and safe delivery to tumor tissues. Moreover, we have established and characterized BMPC cell lines derived from sites of metastasis of MYC-driven transgenic mice with prostate cancer. The allograft tumor models formed by these new prostate cancer cell lines could provide a robust animal platform for the evaluation and screening of drugs and therapeutic NPs. We have also carried out RNAseq experiments on the BMPC and GEM models that will lay the groundwork for deriving our MYC signature that will be used as a pharmacodynamics marker in subsequent studies.

- **What was the impact on other disciplines?**

Nothing to report.

- **What was the impact on technology transfer?**

Nothing to report.

- **What was the impact on society beyond science and technology?**

Nothing to report.

5. CHANGES/PROBLEMS

- **Changes in approach and reasons for change**

Nothing to report.

- **Actual or anticipated problems or delays and actions or plans to resolve them**

Nothing to report.

- **Changes that had a significant impact on expenditures**

Nothing to report.

- **Significant changes in use or care of human subjects, vertebrate animals, biohazards, and/or select agents**

Nothing to report.

- **Significant changes in use or care of human subjects**

Nothing to report.

- **Significant changes in use or care of vertebrate animals**

Nothing to report.

- **Significant changes in use of biohazards and/or select agents**

Nothing to report.

6. PRODUCTS

- **Publications, conference papers, and presentations**

Journal publications:

1. Xu X, Wu J, Liu S, Tao W, Saw PE, Yu M, Li Y, Yegnasubramanian S, De Marzo AM, Shi J, Bieberich CJ, Farokhzad OC. Fast Reduction-Responsive Nanoparticle Platform for Systemic siRNA Delivery and Effective Cancer Therapy. *To be submitted* (Acknowledgement of federal support: yes)
2. Zhu X, Tao W, Liu D, Wu J, Guo Z, Ji X, Bharwani Z, Zhao L, Zhao X, Farokhzad OC, Shi J. Surface De-PEGylation Controls Nanoparticle-Mediated siRNA Delivery In Vitro and In Vivo. **Theranostics** 2017; 7(7):1990-2002. (Acknowledgement of federal support: yes)
3. Shi J, Kantoff PW, Wooster R, Farokhzad OC. Cancer Nanomedicine: Progress, Challenges and Opportunities. **Nat Rev Cancer** 2017; 17:20-37. (Acknowledgement of federal support: yes)
4. Xu X, Wu J, Liu YL, Zhao L, Zhu X, Bhasin S, Li Q, Shi J, Farokhzad OC. Ultra pH-Responsive and Tumor-Penetrating Nanoplatform for Targeted siRNA Delivery with Robust Anti-Cancer Efficacy. **Angew Chem Int Ed** 2016; 55(25):7091-4. (Acknowledgement of federal support: yes)

- **Website(s) or other Internet site(s)**

Nothing to report.

- **Technologies or techniques**

Nothing to report.

- **Inventions, patent applications, and/or licenses**

Nothing to report for Year 2.

- **Other Products**

Nothing to report.

7. PARTICIPANTS & OTHER COLLABORATING ORGANIZATIONS

- **What individuals have worked on the project?**

BWH

Name:	*Omid C. Farokhzad*
Project Role:	*Initiating PI*
Researcher Identifier (e.g. ORCID ID):	
Nearest person month worked:	*0.6*
Contribution to Project:	*Dr. Farokhzad oversees the whole project.*
Funding Support:	

Name:	*Jinjun Shi*
Project Role:	*Co-investigator*
Researcher Identifier (e.g. ORCID ID):	
Nearest person month worked:	*1.2*
Contribution to Project:	*Dr. Shi has supervised the design and development of the hybrid siRNA NPs.*
Funding Support:	

Name:	*Xiaoding Xu*
Project Role:	*Instructor*
Researcher Identifier (e.g. ORCID ID):	
Nearest person month worked:	*12*
Contribution to Project:	*Dr. Xu has lead the siRNA NP development and characterization, polymer synthesis, Pt prodrug synthesis, and in vitro/in vivo testing*
Funding Support:	

Name:	*Yujing Li*
Project Role:	*PhD Student*
Researcher Identifier (e.g. ORCID ID):	*Ms. Li helped Dr. Xu with NP preparation and characterization, and in vitro testing*
Nearest person month worked:	*6*
Contribution to Project:	
Funding Support:	*Chinese Scholarship Council*

JHU

Name:	*Angelo De Marzo*
Project Role:	*Partnering PI*
Researcher Identifier (e.g. ORCID ID):	
Nearest person month worked:	*0.6*
Contribution to Project:	*Dr. De Marzo oversees all experiments at JHU for pathology and sequencing of NP-treated tumor tissues.*
Funding Support:	

Name:	*Srinivasan Yegnasubramanian*
Project Role:	*Co-investigator*
Researcher Identifier (e.g. ORCID ID):	
Nearest person month worked:	*0.6*
Contribution to Project:	*Dr. Yegnasubramanian has supervised the sequencing experiments.*
Funding Support:	

Name:	*Jessica Hicks*
Project Role:	*Technician*
Researcher Identifier (e.g. ORCID ID):	
Nearest person month worked:	*0.6*
Contribution to Project:	*Mrs. Hicks performed IHC assays on the NP treated tissues*
Funding Support:	

UMBC

Name:	*Charles Bieberich*
Project Role:	*Partnering PI*
Researcher Identifier (e.g. ORCID ID):	
Nearest person month worked:	*2*
Contribution to Project:	*Dr. Bieberich oversees all experiments at UMBC to test nanotherapies in BPMC GEM models and in allograft-bearing mice.*
Funding Support:	*Prostate Cancer Foundation*

Name:	*Shuaishuai Liu*
Project Role:	*Graduate student*
Researcher Identifier (e.g. ORCID ID):	
Nearest person month worked:	*6*
Contribution to Project:	*Injection of BMPC cells to generate allograft tumors; injection of RNAi NPs into BMPC GEM and BMPC allograft mice; Western blot analysis of MYC expression*
Funding Support:	

Name:	*Apurv Rege*
Project Role:	*Graduate student*
Researcher Identifier (e.g. ORCID ID):	
Nearest person month worked:	*12*
Contribution to Project:	*Maintenance of BMPC colony; Genotypic analysis of BMPC mice*
Funding Support:	*Prostate Cancer Foundation*

- **Has there been a change in the active other support of the PD/PI(s) or senior/key personnel since the last reporting period?**

Nothing to report.

- **What other organizations were involved as partners?**

We have two partnering organizations in this project.

Partnering PI: Angelo M. De Marzo; Co-I: Srinivasan Yegnasubramanian
Organization Name: The Johns Hopkins University
Organization Location: School of Medicine, 733 N Broadway Baltimore, MD 21205
Partner's Contribution: Collaboration

Partnering PI: Charles J. Bieberich
Organization Name: University of Maryland, Baltimore County
Organization Location: Department of Biological Sciences, 1000 Hilltop Rd, Baltimore, MD 21250
Partner's Contribution: Collaboration

8. SPECIAL REPORTING REQUIREMENTS

➢ COLLABORATIVE AWARDS

This collaborative award is led by Initiating PI (Dr. Farokhzad) and Partnering PIs (Drs. De Marzo and Bieberich). We prepared the report together, and the tasks are clearly marked with the responsible PI and research site as shown in **3. ACCOMPLISHMENTS**.

➢ QUAD CHARTS

Nothing to report.

9. APPENDICES

Nothing to report.